Desalination and Water Treatment
www.deswater.com
doi: 10.5004/dwt.2023.29519

293 (2023) 243–252
May

Investigation of malachite green removal using graphene oxide-zinc oxide composite from aqueous solution: synthesis, characterization and application

Abdulaziz A. Alanazi

Department of Chemistry, College of Science and Humanities in Al-Kharj, Prince Sattam bin Abdulaziz University, Al-Kharj 11942, Saudi Arabia, email: abdulaziz.alanazi@psau.edu.sa

Received 1 November 2022; Accepted 5 April 2023

ABSTRACT

Chemically synthesized graphene oxide-zinc oxide (GO-ZnO) composite was used as an adsorbent to remove malachite green (MG) from the aqueous solution. It was used due to its high thermal stability, high surface area and porous structure which are favourable for adsorption study. Several steps were conducted for the entire research study. GO-ZnO composite was synthesized as an effective adsorbent material. A batch experiment was carried out by using the prepared GO-ZnO adsorbent materials to remove the MG from the aqueous solution. The physicochemical parameters such as pH, contact time, initial concentration and dosage of adsorbent were optimized to get the highest removal efficiency of MG. The maximum removal efficiency of GO-ZnO adsorbent for MG dye was found to be 94% at pH 8. Characterization was carried out to identify the morphology, crystallinity and chemical compositions. The GO-ZnO adsorbent was characterized by using scanning electron microscopy, X-ray photoelectron spectroscopy, X-ray diffraction and Fourier-transform infrared spectroscopy.

Keywords: Graphene oxide; Zinc oxide; Malachite green; Pollutants; Wastewater; Remediation

1. Introduction

In the last few decades, graphene and its associated compounds are developed as a typical class of materials due to their distinctive composition and functional groups [1–3]. Industrial wastewater contains a huge amount of colour effluent from various industrial sources such as synthetic dyes, leather and textiles [4–6]. These effluents are carcinogenic, mutagenic and non-degradable in nature that's why these discharge from wastewater is of great concern [7,8]. These coloured effluents entered directly into water bodies and thus direct inhalation and digestion of effluents severely affect not only aquatic life but also living beings including humans [9,10]. Malachite green is also commonly used to dye fabrics like wool, silk, cotton, and leather. It also functions as a therapeutic antifungal agent in aquaculture, commercial fish hatcheries, and animal husbandry, while for humans it is applied as an antiseptic and fungicidal agent. Furthermore, studies show that the by-products of malachite green's breakdown are unsafe and may cause cancer [11–13]. These effluents are complicated in chemical structure and complex in nature, removal of these effluents is not easy from wastewater by simple methods.

Different techniques were investigated for the removal of these pollutants from contaminated wastewater such as precipitation, flocculation, coagulation, membrane filtration, ion exchange, electrochemical, photo-degradation etc. [13–16]. Out of these techniques, adsorption is regarded to be the most popular, simple, easy, effective and economic method for the expulsion of various contaminants (inorganic and organic) from wastewater treatment plants. Biosorbents, nano clay, carbon nanotubes, and activated carbon are different types of materials which have been used for the adsorption process [17–20]. In wastewater treatment plants

graphene oxide-based composite materials have attracted significant attention because of their large surface areas, more active functionalized sites, and presence of a carboxylic group [21,22]. Graphene-based composites are utilizing as a potential source to make effective and promising adsorbents as compared to other high-cost adsorbents [23,24]. Thus, graphene oxide with metal oxide shows high dispersion in both water and organic solvent due to the presence of the oxygen group. Due to the high values of Young's modulus, high mobility of charge carriers, excellent thermal conductivity, optical transmittance and planar structure graphene oxide form nanocomposite materials with inorganic and polymer materials.

In this article, a graphene oxide-zinc oxide (GO-ZnO) composite was synthesized and applied for the removal of malachite green dye from an aqueous solution. Various physicochemical parameters such as solution pH, contact time, the effect of concentration and dosage effect of composite onto adsorption were optimized.

2. Experimental set-up

2.1. Malachite green and stock solution preparation

All the chemicals were used as analytical rating grades without any further purification. 1,000 mg/L concentration of a stock solution of malachite green (MG) was synthesized by dissolving 1 g of MG in one litre of H_2O. Standards and working solutions were synthesized by further dilutions of stock solution to be used in subsequent experiments. The dye structure is represented in Fig. 1.

A batch adsorption experiment was carried out to optimize the effect of the pH of the solution, initial MG concentration, contact time, and dosage of adsorbent used on the adsorption of MG by using the GO-ZnO composite adsorbent. The initial concentration of MG and the remaining concentration of MG after absorption was measured using a spectrophotometer 617 nm. Table 1 provides a list of malachite green dye characteristics.

2.2. Synthesis of composite material (GO-ZnO)

Graphene oxide particles were synthesized by using a modified Hummer's method [25]. In a conical flask definite amount of conc. HNO_3 and H_2SO_4 (1:2) were added in 1 g graphite powder and were kept up to 24 h demineralized water (DMW) was used to wash the final amount and

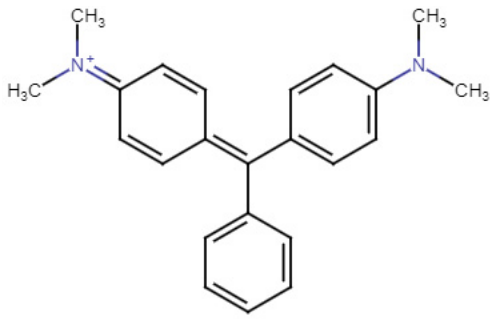

Fig. 1. Chemical structure of malachite green dye molecule.

was dried for some time. The powder obtained was placed in a conical flask (500 mL) and 150 mL of sulphuric acid was added. Next potassium permanganate (2 g) was added slowly with constant stirring. Ice-containing bath was used to maintain the temperature of the reaction mixture (below 20°C) and the reaction mixture was stirred for 6 h. After this DMW (200 mL) was added slowly resulting in the exothermic reaction. Then, hydrogen peroxide (20 mL) was added to the solution and the resulting solution colour changes to yellow-brown. Finally, the resulting solution was centrifuged at 500 rpm and washed with hydrochloric acid and double distilled water to get the product. For the synthesis of GO-ZnO composite, the first 5 g of GO was added into demineralized water (DMW) (100 mL) and was ultrasonicated for about 30 min. Then 100 mL of ZnO solution was added to the solution and sonicated for 15 min. After then, the mixture was vigorously stirred for 12 h and pH 8 was maintained by adding sodium hydroxide. Finally, GO-ZnO composites were obtained after filtering the solution.

2.3. Batch studies

The batch adsorption experiment was conducted to check the removal efficiency of MG onto GO-ZnO composite adsorbent. The statistical graph was plotted using Microsoft Excel.

The percent removal efficiency of MG was determined by the Eq. (1):

$$\text{Removal Efficiency of MG}(\%) = \frac{C_0 - C_e}{C_0} \times 100\% \quad (1)$$

where C_0 = initial concentration of MG before adsorption process (mg/L); C_e = final concentration of MG after adsorption process (mg/L).

2.4. Effect of pH

The effect of pH was carried out by selecting different pH values, which are 2, 3, 4, 5, 6, 7, 8. 9 and 10 and maintaining the solution pH using 0.1 M of NaOH and 0.1 M of HCl. For each run, 100 mg/L of 100 mL MG aqueous solution was prepared and the initial concentration of MG was analysed. 0.1 g of GO-ZnO composite adsorbent dosage was weighed and placed in a beaker that contained MG solution. The suspension was stirred for two 2 h at room temperature by using a magnetic stirrer. Then, the MG solution was analysed after the adsorption process using a spectrophotometer.

2.5. Effect of contact time

The effect of contact time was carried out on different time intervals 15, 30, 45, 60, 90, 120, 150, and 180 min with the optimized pH. For each run, 100 mg/L of MG dye in a 100 mL volume of the aqueous solution was prepared and the initial concentration of MG was analysed. 0.1 g of GO-ZnO composite adsorbent dosage was weighed and placed in the flask that contained MG solution. The suspension was stirred by using a magnetic stirrer at room temperature

with different contact times. Then, the concentration of the MG solution was measured by spectrophotometer.

2.6. Effect of initial concentration of MG solution

The effect of the initial concentration of MG solution was carried out by selecting varied concentration range 10, 20, 40, 60, 80, 100, 125, and 150 mg/L in 100 mL of MG solution with optimized pH and contact time. For each run, the initial concentration of MG was analysed. 0.1 g of GO-ZnO composite adsorbent dosage was weighed and placed in the flask that contained MG solution. The suspension was stirred by using a magnetic stirrer at room temperature. Then, some amount of MG solution was taken and the final concentration of MG solution was measured by spectrophotometer.

2.7. Effect of amount of adsorbent

The GO-ZnO composite adsorbent dosage was varied from 0.025, 0.05, 0.075, 0.1, 0.125, 0.15 and 0.2 g to check the effect of adsorbent dosage on the adsorption process. For each run, 100 mg/L MG aqueous solution was prepared. The initial concentration of MG was analysed. The GO-ZnO composite adsorbent dosage was weighed and placed in the prepared MG solution. The suspension was stirred by using a magnetic stirrer and magnetic bar at speed of 200 rpm with optimized parameters pH, time and concentration. After the adsorption process, the final concentration of MG solution was measured by spectrophotometer.

3. Results and discussion

3.1. Characterization of GO-ZnO composite adsorbent

3.1.1. Scanning electron microscopy

Scanning electron microscopy (SEM) was used for the investigation of the morphology of GO-ZnO before and after the adsorption of malachite green. Fig. 2a shows cavities and irregular and porous structures on the surface of the GO-ZnO adsorbent. After adsorption of malachite green dye, the GO-ZnO surface is changed, and cavities and pores are filled with malachite green dye as in Fig. 2b. The adsorption of malachite green on GO-ZnO surface mainly depends on cavities and multi-porous surfaces. Similar results were reported by Hosseini et al. [26].

3.1.2. Fourier-transform infrared spectroscopy

Fourier-transform infrared (FTIR) spectra were recorded in the range of 400–4,000 cm^{-1} to identify the functional group present on the surface of GO-ZnO adsorbent (Fig. 3a and b). The spectrum of GO-ZnO adsorbent is shown in Fig. 3a. The peak obtained at 3,320 cm^{-1} may be attributed to the –OH stretching vibration of the hydroxyl group (OH) of the graphene oxide unit. The peaks at 1,730 and 1,086 cm^{-1} may correspond to carbonyl group (C=O) and C–O group of the carboxylic acid group of graphene oxide. The peaks appear in the range 672 cm^{-1} correspond to the metal oxide (Zn–O) group. After the adsorption of dye molecules onto GO-ZnO, some shifts (20–30 cm^{-1}) were observed in the hydroxyl and carboxylic groups which confirms that these functional groups are responsible for adsorption [27].

3.1.3. X-ray photoelectron spectra of GO-ZnO

The GO-ZnO composite's chemical state and composition may be better understood using a important characterization technique like X-ray photoelectron spectroscopy (XPS). The XPS spectra of GO-ZnO are presented in Fig. 4. According to the survey spectrum in Fig. 4a, the main elements are Zn, O, and C. The Zn 2p spectrum is shown in Fig. 3b, with two bands at 1,047.0 and 1,025.4 eV, which correspond to Zn 2p1/2 and Zn 2p3/2 in ZnO, respectively [28]. As shown in Fig. 4c, the C 1s spectra peak appeared at 289.7,

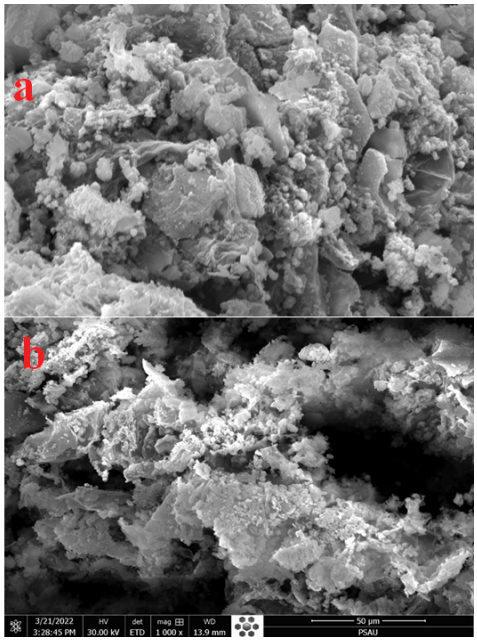

Fig. 2. Scanning electron microscopy image of (a) GO-ZnO adsorbent before dye adsorption and (b) GO-ZnO based adsorbent after adsorption of malachite green dye.

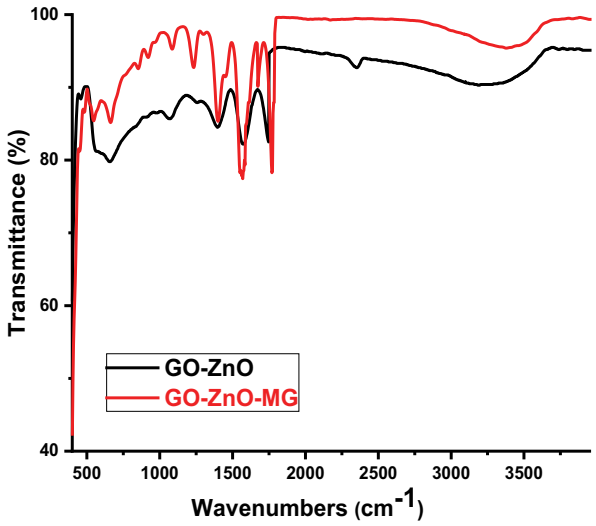

Fig. 3. Fourier-transform infrared spectra of (a) GO-ZnO composite adsorbent before malachite green adsorption and (b) GO-ZnO adsorbent after malachite green adsorption.

which correspond to the GO functional group (C=O). Lattice oxygen (OL) of ZnO and functional group (C=O) of GO, may be appeared at 535.8 in the O 1s XPS peak exhibited in Fig. 4d.

3.1.4. BET surface analysis

In the current study, the GO-ZnO composite's BET surface analysis was carried out using Quantachrome® ASiQwin™-Instruments (version 5.0). Pore size, surface area, and volume of composite play significant role in the adsorption process. Using nitrogen adsorption–desorption (BET) technique, the GO-ZnO composite is analysed. From the results, surface area, pore volume and pore radius of composite material are 25.891 m^2/g, 0.275 cc/g and 19.142 Å, respectively.

3.1.5. X-ray diffraction spectrum of GO-ZnO

The (110), (002), (101), (102), (110), (103), (112), (201), and (202) crystalline planes of ZnO are represented by the peaks at 32, 34, 6, 36.4, 47, 8, 56, 63, 68, 3, 69.53, and 77.5 in the X-ray diffraction (XRD) pattern of the ZnO nanoparticles (Fig. 5a). The major peaks of the XRD pattern for the GO/ZnO nanocomposite are shown in Fig. 5b. The XRD pattern of the nanocomposite exhibits the principal ZnO peaks, and the diffraction peaks of the GO/ZnO nanocomposite are similar to those of ZnO nanoparticles. The peak at 2Ø = 10° is ascribed to the graphene oxide nanosheet. The GO peak in the nanocomposite suggests that the sheets could have been restacked. It appeared around the 2Ø = 12° but it is in restacked position therefore, it's not appeared as broad peak. Similar, the peak at 2Ø = 29° indicated the ZnO presence in the composite but after the absorption it moved to 2Ø = 31°. According to the literature, GO sheet are detected between 2Ø = 10° to 12° and ZnO presence can be at 2Ø = 31° [29,30]. Its mean that there is no obvious change in the diffraction pattern of GO-ZnO after adsorption of MG, which suggests that the primary mechanism of removal is adsorption of MG onto the surface of GO-ZnO rather than intercalation

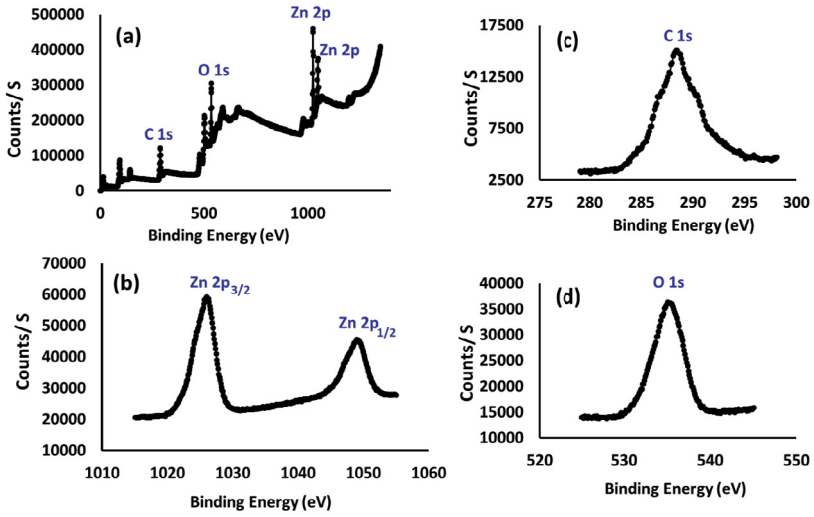

Fig. 4. Spectra of X-ray photoelectron spectroscopy of composite (GO-ZnO) (a) survey scan, (b) Zn 2p, (c) C 1s, and (d) O 1s.

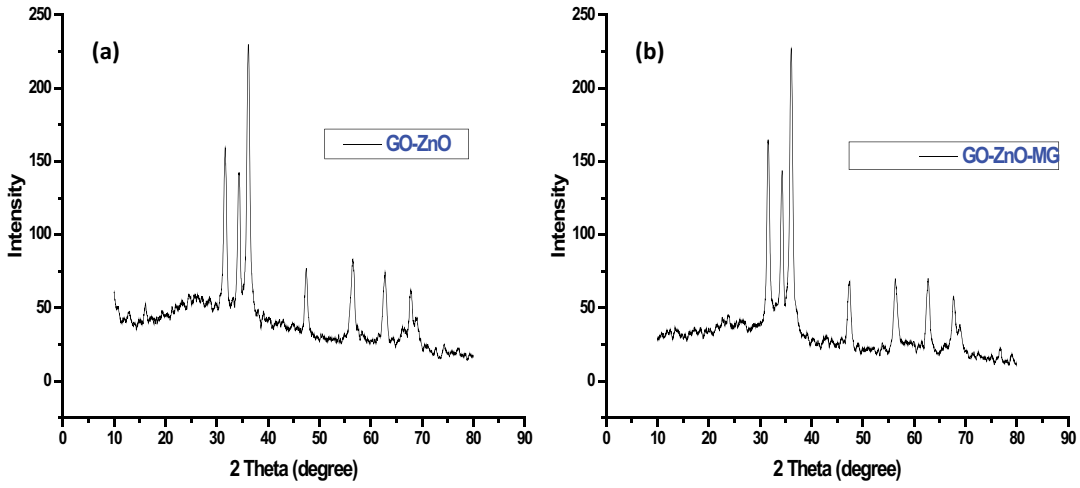

Fig. 5. X-ray diffraction pattern of (a) GO-ZnO composite and (b) GO-ZnO-MG.

in the interlayer of the GO-ZnO. This is because intercalation in the GO-ZnO would cause a change in the diffraction pattern, which would be visible.

3.2. Effect of solution pH on adsorption of dye and point zero charge (PZC)

The removal efficiency of dye mainly depends on pH. Adsorption of malachite green onto GO-ZnO was done and studied by varying the pH from 2 to 10. At pH 8 maximum removal efficiency was achieved (about 94%) as in Fig. 6. Malachite green is cationic in therefore, the highest removal efficiency was achieved in basic pH due to satisfactory conditions for GO-ZnO surface and malachite green dye due to the strong electrostatic force of attraction between negatively charged GO-ZnO adsorbent and positively charged malachite green dye molecules. In acidic medium low removal efficiency was obtained due to an increase in a number of positive charge on the surface of GO-ZnO adsorbent which repels the positively charged malachite green dye molecules. Similar results were reported by Muinde et al. [31].

When the surface charge of the adsorbent is zero, a physical phenomenon known as the point of zero charge (PZC) of adsorption occurs. The pH_{PZC} is affected by a number of variables such as type of adsorbents used, temperature, the number of impurities present, and how well analyte adsorb. The solid addition approach was used to conduct this experiment. The exact amount of 50 mL of a 0.01 M NaCl solution was transferred to a flask, and the pH of the solution was then adjusted (within the range of 2–10) using 0.1 M HCl or NaOH solution. After that, 0.1 g of GO-ZnO composite material was transferred into each flask and being swirled for 24 h with the help of magnetic stirrer. The final pH of solution after stirring was recorded. The graph of pH_i and pH_f was plotted (Fig. 7). The curve revealed that the pH of the solution was above the isoelectric point (pH_{pzc} 6.6), which caused a significant accumulation of negative charge on the GO-ZnO composite surface and promoted the adsorption of positively charged dye [32].

3.3. Effect of contact time and linear and non-linear kinetic models

100 mg/L of malachite green dye in 100 mL and 0.1 g GO-ZnO adsorbent dosage was used to study the effect of contact time on the adsorption of malachite green dye at different times 15, 30, 60, 90, 120, 150 and 180 min. Fig. 8 shows the relationship between contact time and dye removal efficiency. The adsorption rate on the surface of GO-ZnO adsorbent is faster initially and then due to internal diffusion phenomena adsorption rate slows down. This is due to the rate-determining step. After 60 min, the same removal efficiency was observed. Therefore, the time required to reach equilibrium was 60 min for the malachite green dye. A similar result is reported by Arivoli et al. [33].

In order to carrying out adsorption activities, the kinetic parameters are useful in determining the rate of adsorption. The pseudo-first and second models' kinetic factors were applied to recognize the kinetic of MG dye adsorption onto GO-ZnO composite [34].

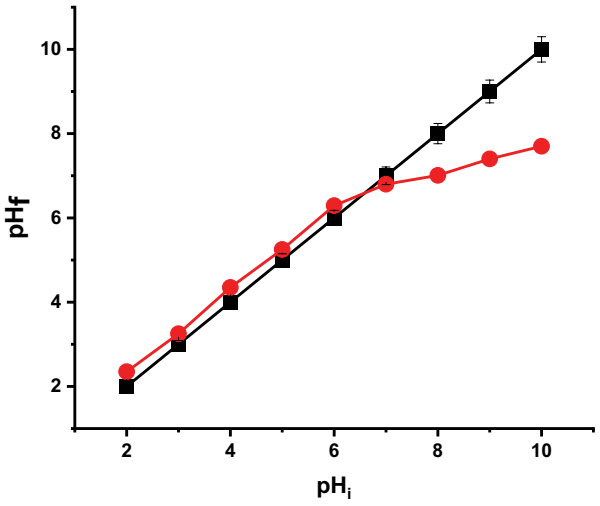

Fig. 7. Point of zero charge study of GO-ZnO composite surface.

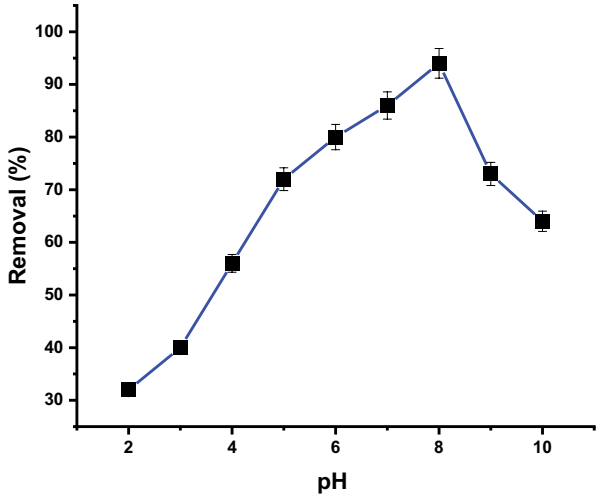

Fig. 6. Graph of removal efficiency of malachite green (%) vs. solution pH (malachite green concentration 100 mg/L, adsorbent dosage = 0.1 g, time = 180 min).

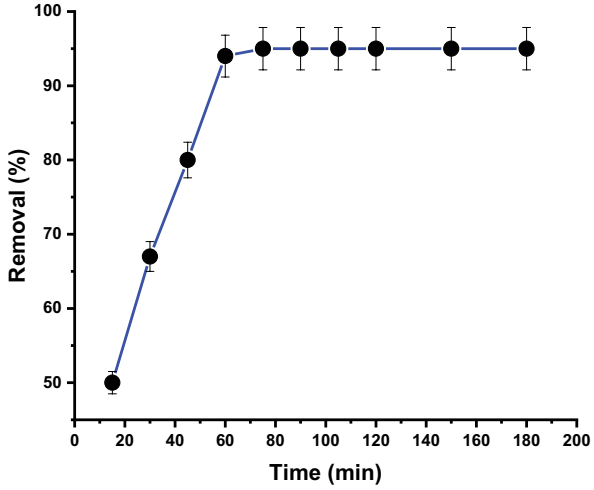

Fig. 8. Graph of removal efficiency of malachite green (%) vs. time (min) (malachite green concentration 100 mg/L, adsorbent dosage = 0.1 g, pH = 8).

First-order represents as:

$$\log\left(q_e - q_t\right) = \log q_e - \frac{k_1 t}{2.303} \quad (2)$$

Second-order represents as:

$$\frac{t}{q_t} = \frac{1}{k_2 q_e^2} + \frac{t}{q} \quad (3)$$

where k_1 and k_2 are first- and second-order rate constants, respectively. The terms q_e and q_t refer to the adsorption capacity (mg/g) of MG at equilibrium at the relevant times, t. The kinetic model factors were calculated and tabulated in Table 2. The value of q_e was shown to be more accurately fitted by the pseudo-second-order and to be closer to the value of the experimental data of GO-ZnO. For second-order kinetics, the regression coefficient value (R^2-0.9924) is higher than the regression coefficient value (R^2-0.8831) of first-order kinetics model. Similar results were observed by Özbaş et al. [35] which is comparable with current study findings.

To comprehend better adsorbents and create the perfect adsorption system, the most appropriate non-linear kinetic models must be determined. For accurate prediction, these mathematical models must be studied of the variables and constants in adsorption process. They are essential for streamlining the routes of the adsorption mechanism. To effectively develop adsorption systems and express the surface capabilities of adsorbents, models must be researched [36]. Non-linear kinetic models was represented as Fig. 9 and data was tabulated in Table 2.

The pseudo-first-order non-linear model's ability to directly compute equilibrium sorption capacity (q_e) from the course of adsorption over time overcomes a significant drawback of the pseudo-first-order linear model's application, which is that such adsorption capacity must first be experimentally established [37].

As a result, the experimental equilibrium adsorption capacity ($q_{e,exp}$) in the current study was closer than the calculated equilibrium adsorption ($q_{e,cal}$), considerably lower the Chi-square tabular value (0.3562). According to our findings, greater linear regression coefficient was obtained, the equilibrium adsorption capacity was good fitted as compared to linear model was applied to the adsorption kinetics.

Table 1
Physical properties of malachite green dye

Properties	Values
Nature	Cationic dye
Chemical formula	$C_{23}H_{25}ClN_2$
IUPAC name	[4-[4-(dimethylamino)phenyl]-phenyl-methylidene]cyclohexa-2,5-di-en-1-ylidene]-dimethylazanium; chloride
Molecular weight	364.911
(λ) max	617 nm

Results of pseudo-second-order exhibited two values were comparably but Chi-square tabular value (1.8807) higher than the pseudo-first-order and lower linear regression coefficients (R^2 0.9383). In comparison between experimental and calculated adsorption at equilibrium, it was suggested that the pseudo-first-order non-linear model's fit the data better than the non-linear pseudo-second-order. A very low Chi-square test result indicates that calculated data match experimental data very well.

3.4. Effect of initial concentration of MG and isotherm studies

Removal efficiency depends on the initial concentration of dye. Initially, effect of malachite green dye concentration was studied in the range of 10–150 mg/L under optimized conditions, pH 8, time 60 min and 0.1 g adsorbent dosage. The result is shown in Fig. 10. It can be observed from the figure that the removal efficiency of malachite green onto GO-ZnO initially increases with an increase in the concentration of dye which may be due to the presence of free active sites. After some time, no significant change was observed in the removal efficiency and finally decrease in removal efficiency was observed with a further increase in the

Table 2
Kinetic model parameters for adsorption of malachite green onto GO-ZnO composite

Linear kinetics			
Pseudo-first-order model		Pseudo-second-order model	
$q_{e(cal)}$ (mg/g)	65.96	$q_{e(cal)}$ (mg/g)	120.48
k_1 (min^{-1})	0.066	k_2 (g/(mg·min))	0.00039
R^2	0.8831	R^2	0.9924
Non-linear kinetics			
q_e (mg/g)	96.22	q_e (mg/g)	109.74
k_1 (min^{-1})	0.041	k_2 (g/(mg·min))	0.00050
R^2	0.9871	R^2	0.9383
Chi-square	0.3562	Chi-square	1.8807

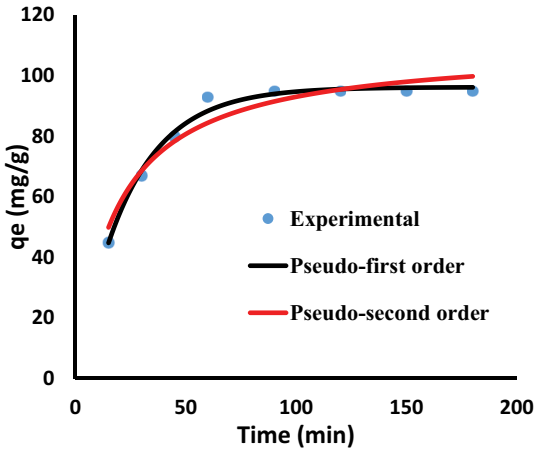

Fig. 9. Non-linearized form of pseudo-first-order and pseudo-second-order kinetics model.

concentration of malachite green dye. Similar results were reported by Guo et al. [34].

By using different adsorption isotherms, such as the Langmuir isotherm and Freundlich isotherm model, the equilibrium of varied dye concentrations is well identified. In this work, different concentration of malachite green dye (10–150 g/mL) were used. The Freundlich isotherm occurs on the heterogeneity of adsorbents, whereas the Langmuir model assumes that adsorption proceeds through various functional groups present on the surface of GO-ZnO adsorbent and predicts monolayer with homogenous active sites. The following equation [38] reports the linearized form of models like the Freundlich isotherm and Langmuir model.

$$\frac{C_e}{q_e} = \frac{1}{q_m b} + \frac{C_e}{q_m} \tag{4}$$

$$\ln q_e = \ln K_f + \frac{1}{n}\ln C_e \tag{5}$$

Above given expressions, the adsorbed amount of dye at equilibrium is denoted by q_e (mg/g), the dye equilibrium concentration is denoted by C_e (mg/L), and q_m and b denotes the Langmuir adsorption efficiency and constants, respectively. K_f and n value denote the Freundlich constant. The linear plot of the Langmuir isotherm, represented by the plot C_e/q_e vs. C_e, was plotted. The calculated values based on the intercept and slope are tabulated in Table 3. From the results, we can see that q_m value (monolayer adsorption capacity) is more favourable due to homogeneous distribution of active sites as compared to multilayer adsorption (Freundlich adsorption capacity) on the GO-ZnO surface. Regression coefficient is also high (R^2-0.9997) in case of Langmuir isotherm. The occurrence of adsorption process was designated by the R_L constant and its ranged from 0 to 1. In this study, the R_L constant was found to be 0.196, which is within the range. This demonstrated that adsorption was favourable [39]. Similar results were observed by different studies which is comparable with current study findings [40–42].

Adsorption isotherms show the physical and chemical interactions that were formed during the incubation process between the adsorbate and the surface of adsorbents. According to published research, linear studies and non-linear equilibrium modelling have emerged as the most effective techniques for assessing adsorption characteristics. In the current work, coupled error analysis has been applied using isotherms models of two and three parameters. Based on the regression coefficient, Chi-square, and calculated q_e value, the optimal isotherm model that matches the experimental data is selected. Non-linearized form of Langmuir and Freundlich model was represented in Fig. 11 and data is tabulated in Table 3.

The tendency of the Freundlich model to better fit data at low experimental concentrations and the Langmuir model to better fit data at higher experimental concentrations are examples of bias that may result from the transformation of non-linear equations to linear forms in isotherm

Table 3
Langmuir and Freundlich isotherm for the adsorption of malachite green onto GO-ZnO composite

Linear isotherm			
Langmuir isotherm		Freundlich isotherm	
q_m (mg/g)	104.16	K_f (mg/g)(L/mg)$^{1/n}$)	10.33
b (L mg−1)	0.854	n	1.52
R^2	0.9997	R^2	0.9407
R_L	0.196		
Non-linear isotherm			
q_e (mg/g)	129.87	K_f ((mg/g)(L/mg)$^{1/nfr}$)	14.70
K_l (L/mg)	0.059	n (dimensionless)	2.04
R^2	0.8743	R^2	0.7724
Chi-square	25.86	Chi-square	41.74

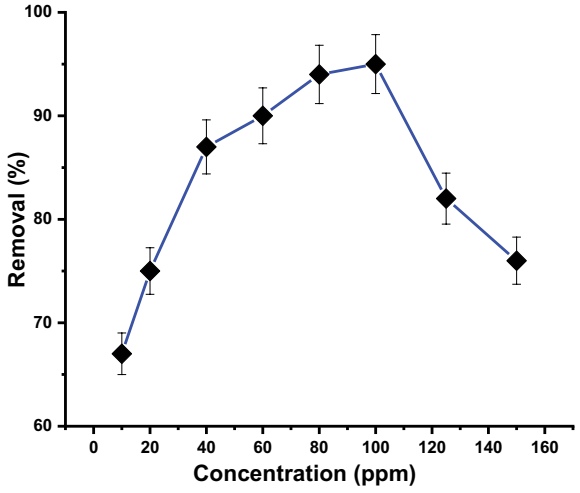

Fig. 10. Graph of removal efficiency of malachite green (%) vs. initial concentration of malachite green solution (mg/L) (adsorbent dosage = 0.1 g, pH 8 and time = 60 min).

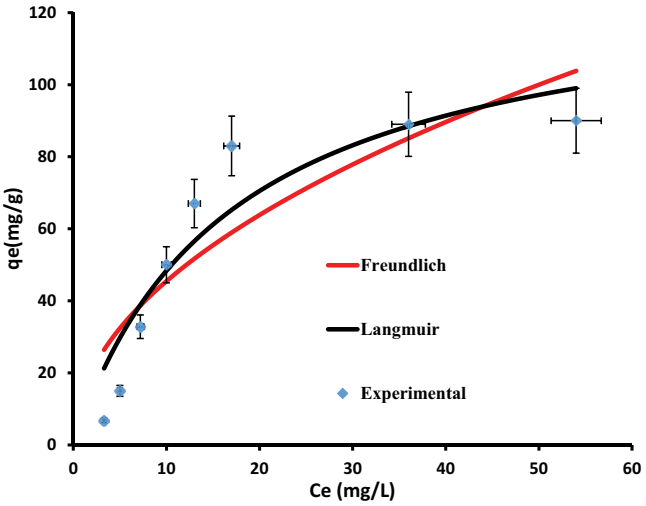

Fig. 11. Non-linearized form of Langmuir and Freundlich model.

models [43]. From the results, the experimental equilibrium adsorption capacity ($q_{e,\exp}$) in the Langmuir model was closer than the calculated equilibrium adsorption ($q_{e,\text{cal}}$), considerably lower the Chi-square tabular value (25.86) as compared to Freundlich isotherm (41.74). According to our findings, greater linear regression coefficient (0.8743) was obtained in case of Langmuir model.

3.5. Thermodynamic parameters for the adsorption

The following equations were used to determine the free energy change ($G°$), entropy change ($S°$), and enthalpy change ($H°$) for the adsorption process of dye removal:

$$\Delta G° = -RT\ln K_c \tag{6}$$

$$\ln K_c = \frac{\Delta S°}{R} - \frac{\Delta H°}{RT} \tag{7}$$

where T (K) is the absolute temperature, R = (8.314 J·mol·K) which is universal gas constant. K_c is the distribution coefficient.

The degree of the enthalpy change ($H°$) and entropy change ($S°$) can be used to categorize the type of interaction between the adsorbent and adsorbate. At various experimental temperatures (298–333 K), the adsorption of MG onto GO-ZnO adsorbent was evaluated using the gradient and intercept of the logK_d vs. 1/T curve, as shown in Fig. 12. Table 4 shows that as temperature climbed from 298 to 333 K, $G°$ values varied from –5.599 to –7.835 kJ/mol, and the –ve value of $G°$ may be attributed to the feasibility and spontaneity of the adsorption process with improved sorption efficacy of MG on GO-ZnO adsorbent. In general, physiosorption is indicated by a change in adsorption enthalpy between –20 and 40 kJ/mol, and chemisorption is indicated by a change between –400 and –80 kJ/mol [44]. A positive $H°$ (36.95 kJ/mol) indicates an endothermic reaction and physical adsorption, according to experimental data. Hence, the outcome demonstrated that physical forces were involved in the MG's adsorption onto the GO-ZnO adsorbent.

Also, the enhanced disorderliness of the solid–liquid interfacial contact during the adsorption process of dye (MG) onto GO-ZnO is suggested by the positive values of $S°$ (67.85 kJ/mol·K) [45].

3.6. Effect of amount of adsorbent

The effect of the amount of adsorbent for the removal of malachite green dye was done by using different amounts of dosage (0.05–0.20 g) of GO-ZnO adsorbent material under optimized conditions (pH 8, 100 mg/L dye concentration and 60 min). Fig. 13. shows the effect of the amount of adsorbent on the removal of malachite green dye. It can be investigated from the figure that due to a high number of active sites present on adsorbent removal efficiency of malachite green dye increases initially with the increase in the amount of GO-ZnO adsorbent material. Removal efficiency remains constant from 0.1 to 0.2 g maybe due to the agglomeration or aggregation of adsorbent which leads to a decrease in active surface sites. The removal efficiency was achieved at 94% when 0.1 g of adsorbent was used for the removal of dye in an aqueous solution. A similar result was summarized by Kiani et al. [46].

Table 4
Thermodynamic experiment for the adsorption of malachite green onto GO-ZnO composite

$\Delta H°$ (kJ/mol)	$\Delta S°$ (kJ/mol·K)	Temperature (K)	$\Delta G°$ (kJ/mol)
36.95	67.85	298	–5.599
		313	–6.296
		323	–7.089
		333	–7.835

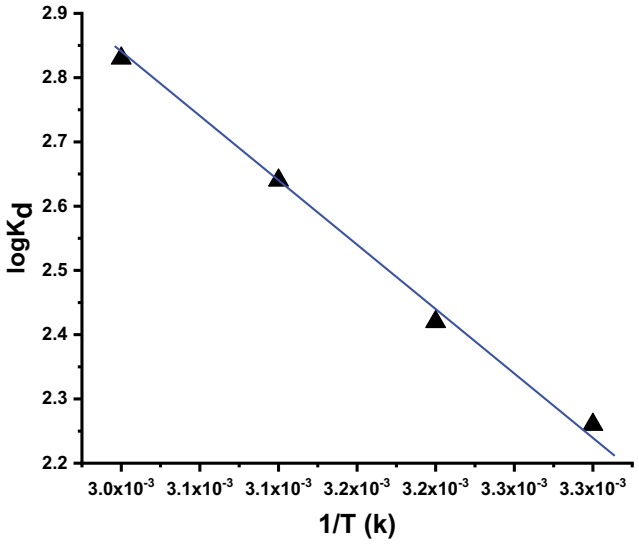

Fig. 12. Van't Hoff plot for adsorption of malachite green onto GO-ZnO composite.

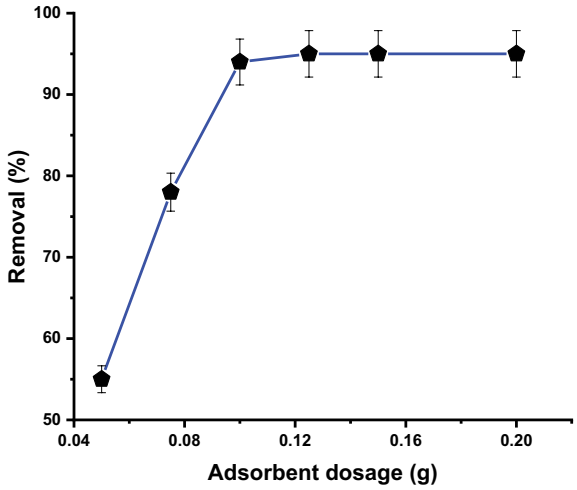

Fig. 13. Graph of removal efficiency of malachite green (%) vs. the amount of adsorbent used (g) (malachite green concentration 100 mg/L, pH 8 and time = 60 min).

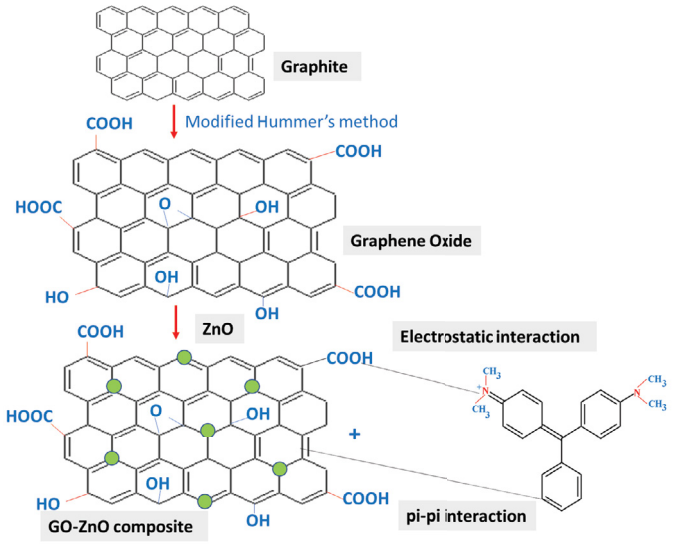

Fig. 14. Interaction mechanism of malachite green dye onto GO-ZnO adsorbent surface.

3.7. Regeneration capacity of GO-ZnO

Using various acids ((hydrochloric acid, nitric acid, sulfuric acid), MG saturated adsorbent regeneration was carried out. Adsorption of MG dyes with a concentration of 100 mg/L was taken by using 0.1 g of adsorbent materials for desorption study. Adsorbent that had been saturated with dye was fixed in a column after adsorption. Each acid (20 mL of 0.1 M) was employed to elute the dye from the adsorbents. According to the findings, using three different acids—hydrochloric acid, nitric acid and, sulfuric acid, the desorption rate percentage was found satisfactory up to 5 cycles, After 5 cycles, adsorbent loose its capacity by 20%–30%. In this investigation, hydrochloric acid performs more effectively than the other acids used in this experiment.

3.8. Possible interaction mechanism of GO-ZnO surface with MG

Fig. 14 shows the assembly of malachite green dye on the GO-ZnO surface. Different groups like hydroxyl, epoxy and carboxylic are present on the surface of graphene oxide. The binding or adsorption of malachite green on GO-ZnO is due to the presence of these groups. Malachite green is a cationic dye and GO-ZnO in a basic medium (pH 8) is negatively charged which promotes interaction between malachite green dye and GO-ZnO surface functional groups [42]. Another probability of interaction is due to electrostatic, π-π interaction and H-bonding between malachite green dye and GO-ZnO.

4. Conclusions

The batch adsorption method was used for the removal of malachite green using GO-ZnO adsorbent. The results were obtained under the optimized condition of initial concentration, pH, solution, amount of adsorbent and contact time, 100 mg/L, 8, 0.1 g and 60 min, respectively. FTIR, XPS, XRD and SEM spectra of GO-ZnO adsorbent confirm the rough and spongy surface, the functional group, crystallinity associated with GO-ZnO, effective for malachite green dye removal. Moreover, the maximum removal efficiency of malachite green onto GO-ZnO adsorbent was 94%. GO-ZnO adsorbent material could be an alternative adsorbent for the removal of pollutants from industrial wastewater due to its high surface area, high thermal stability and high removal efficiency.

Acknowledgments

This study is supported via funding from Prince Sattam bin Abdulaziz University project number (PSAU/2023/R/1444).

References

[1] A.T. Dideikin, A.Y. Vul, Graphene oxide and derivatives: the place in graphene family, Front. Phys., 6 (2019) 149, doi: 10.3389/fphy.2018.00149.
[2] A.K. Geim, K.S. Novoselov, The Rise of Graphene, Nanoscience and Technology: A Collection of Reviews From Nature Journals, World Scientific Publishing, Singapore, 2010, pp. 11–19.
[3] X. Huang, Z. Yin, S. Wu, X. Qi, Q. He, Q. Zhang, Q. Yan, F. Boey, H. Zhang, Graphene-based materials: synthesis, characterization, properties, and applications, Small, 7 (2011) 1876–1902.
[4] A. Soltani, M. Faramarzi, S.A.M. Parsa, A review on adsorbent parameters for removal of dye products from industrial wastewater, Water Qual. Res. J., 56 (2021) 181–193.
[5] D.A. Yaseen, M. Scholz, Textile dye wastewater characteristics and constituents of synthetic effluents: a critical review, Int. J. Environ. Sci. Technol., 16 (2019) 1193–1226.
[6] S. Rafaqat, N. Ali, C. Torres, B. Rittmann, Recent progress in the treatment of dyes wastewater using microbial-electro-Fenton technology, RSC Adv., 12 (2022) 17104–17137.
[7] K. Golka, S. Kopps, Z.W. Myslak, Carcinogenicity of azo colorants: influence of solubility and bioavailability, Toxicol. Lett., 151 (2004) 203–210.
[8] S. Kobylewski, M.F. Jacobson, Toxicology of food dyes, Int. J. Occup. Environ. Health, 18 (2012) 220–246.
[9] B. Lellis, C.Z. Fávaro-Polonio, J.A. Pamphile, J.C. Polonio, Effects of textile dyes on health and the environment and bioremediation potential of living organisms, Biotechnol. Res. Innovation, 3 (2019) 275–290.

[10] M. Berradi, R. Hsissou, M. Khudhair, M. Assouag, O. Cherkaoui, A. El-Bachiri, A. El-Harfi, Textile finishing dyes and their impact on aquatic environs, Heliyon, 5 (2019) e02711, doi: 10.1016/j.heliyon.2019.e02711.
[11] C. Aroraa, P. Kumara, S. Sonia, J. Mittal, A. Mittal, B. Singh, Efficient removal of malachite green dye from aqueous solution using *Curcuma caesia* based activated carbon, Desal. Water Treat., 195 (2020) 341–352.
[12] A. Mittal, Adsorption kinetics of removal of a toxic dye, Malachite Green, from wastewater by using hen feathers, J. Hazard. Mater., 133 (2006) 196–202.
[13] A. Mittal, L. Krishnan, V.K. Gupta, Removal and recovery of malachite green from wastewater using an agricultural waste material, de-oiled soya, Sep. Purif. Technol., 43 (2005) 125–133.
[14] K. Piaskowski, R. Świderska-Dąbrowska, P.K. Zarzycki, Dye removal from water and wastewater using various physical, chemical, and biological processes, J. AOAC Int., 101 (2018) 1371–1384.
[15] V. Katheresan, J. Kansedo, S.Y. Lau, Efficiency of various recent wastewater dye removal methods: a review, J. Environ. Chem. Eng., 6 (2018) 4676–4697.
[16] S.S. Muthu, A. Khadir, Advanced Removal Techniques for Dye-containing Wastewaters, S.S. Muthu, A. Khadir, Eds., Sustainable Textiles: Production, Processing, Manufacturing & Chemistry, Chemistry and Materials Science, Chemistry and Material Science (R0), Springer, Singapore, 2021, pp. 1–283.
[17] F. Mashkoor, A. Nasar, Inamuddin, Carbon nanotube-based adsorbents for the removal of dyes from waters: a review, Environ. Chem. Lett., 18 (2020) 605–629.
[18] T.A. Aragaw, F.M. Bogale, Biomass-based adsorbents for removal of dyes from wastewater: a review, Front. Environ. Sci., 9 (2021) 764958, doi: 10.3389/fenvs.2021.764958.
[19] V.K. Gupta, A. Mittal, L. Krishnan, V. Gajbe, Adsorption kinetics and column operations for the removal and recovery of malachite green from wastewater using bottom ash, Sep. Purif. Technol., 40 (2004) 87–96.
[20] J. Mittal, Recent progress in the synthesis of layered double hydroxides and their application for the adsorptive removal of dyes: a review, J. Environ. Manage., 295 (2021) 113017, doi: 10.1016/j.jenvman.2021.113017.
[21] I. Ali, A.A. Basheer, X.Y. Mbianda, A. Burakov, E. Galunin, I. Burakova, E. Mkrtchyan, A. Tkachev, V. Grachev, Graphene based adsorbents for remediation of noxious pollutants from wastewater, Environ. Int., 27 (2019) 160–180.
[22] G.K. Ramesh, A. Vijaya Kumar, H.B. Muralidhar, S. Sampath, Graphene and graphene oxide as effective adsorbents toward anionic and cationic dyes, J. Colloid Interface Sci., 361 (2011) 270–277.
[23] H. Hu, W. Wen, J.Z. Ou, Construction of adsorbents with graphene and its derivatives for wastewater treatment: a review, Environ. Sci. Nano, 9 (2022) 3226–3276.
[24] R. Allgayer, N. Yousefi, N. Tufenkji, Graphene oxide sponge as adsorbent for organic contaminants: comparison with granular activated carbon and influence of water chemistry, Environ. Sci. Nano, 7 (2020) 2669–2680.
[25] A. Annisa, R. Mutiara, C.G. Afrilia, A. Bahtiar, S. Suryaningsih, L. Safriani, Preliminary study of ZnO/GO composite preparation as photocatalyst material for degradation methylene blue under low UV-light irradiation, Mater. Sci. Forum, 1028 (2021) 319–325.
[26] S.A. Hosseini, S. Mashaykhi, S. Babaei, Graphene oxide/zinc oxide nanocomposite: a superior adsorbent for removal of methylene blue-statistical analysis by response surface methodology (RSM), S. Afr. J. Chem., 69 (2016) 105–112.
[27] P. Banerjee, A. Mukhopadhayay, P. Das, Ultrasound enhanced azo dye adsorption by graphene oxide nanocomposite, Madridge J. Nanotechnol. Nanosci., 3 (2018) 106–111.
[28] G. Qu, G. Fan, M. Zhou, X. Rong, T. Li, R. Zhang, J. Sun, D. Chen, Graphene-modified ZnO nanostructures for low-temperature NO_2 sensing, ACS Omega, 4 (2019) 4221–4232.
[29] O. Moradi, A. Pudineh, S. Sedaghat, Synthesis and characterization Agar/GO/ZnO NPs nanocomposite for removal of methylene blue and methyl orange as azo dyes from food industrial effluents, Food Chem. Toxicol., 169 (2022) 113412, doi: 10.1016/j.fct.2022.113412.
[30] G. Kiani, M. Dostali, A. Rostami, A.R. Khataee, Adsorption studies on the removal of malachite green from aqueous solutions onto halloysite nanotubes, Appl. Clay Sci., 54 (2011) 34–39.
[31] V.M. Muinde, J.M. Onyari, B. Wamalwa, J.N. Wabomba, Adsorption of malachite green dye from aqueous solutions using mesoporous chitosan–zinc oxide composite material, Environ. Chem. Ecotoxicol., 2 (2020) 115–125.
[32] A. Ahmad, D. Lokhat, M. Rafatullah, A. Khatoon, S.H.M. Setapar, Aloe vera biomass containing cellulosic moieties used as sustainable adsorbents for the removal of crystal violet dye from aqueous solution, Desal. Water Treat., 170 (2019) 337–348.
[33] S. Arivoli, M. Hema, P. Prasath, M. Deva, Adsorption of malachite green onto carbon prepared from borassus bar, Arabian J. Sci. Eng., 34 (2009) 31–42.
[34] F. Guo, X. Jiang, X. Li, X. Jia, S. Liang, L. Qian, Synthesis of MgO/Fe_3O_4 nanoparticles embedded activated carbon from biomass for high-efficient adsorption of malachite green, Mater. Chem. Phys., 240 (2020) 122240, doi: 10.1016/j.matchemphys.2019.122240.
[35] E.E. Özbaş, B. Balçık, H.K. Ozcan, Preparation of activated carbon from waste tires, and its use for dye removal, Desal. Water Treat., 172 (2019) 78–85.
[36] K. Suwannahong, S. Wongcharee, T. Kreetachart, C. Sirilamduan, J. Rioyo, A. Wongphat, Evaluation of the Microsoft Excel Solver spreadsheet-based program for non-linear expressions of adsorption isotherm models onto magnetic nanosorbent, Appl. Sci., 11 (2021) 7432, doi: 10.3390/app11167432.
[37] Y.S. Ho, G. McKay, A comparison of chemisorption kinetic models applied to pollutant removal on various sorbents, Process Saf. Environ. Prot., 76 (1998) 332–340.
[38] M.I. El-Khaiary, G.F. Malash, Common data analysis errors in batch adsorption studies, Hydrometallurgy, 105 (2011) 314–320.
[39] K.Y. Foo, B.H. Hameed, Insights into the modeling of adsorption isotherm systems, Chem. Eng. J., 156 (2010) 2–10.
[40] J. Mittal, R. Ahmad, A. Mittal, Kahwa tea (*Camellia sinensis*) carbon — a novel and green low-cost adsorbent for the sequestration of Titan yellow dye from its aqueous solutions, Desal. Water Treat., 227 (2021) 404–411.
[41] A. Patel, S. Soni, J. Mittal, A. Mittal, C. Arora, Sequestration of crystal violet from aqueous solution using ash of black turmeric rhizome, Desal. Water Treat., 220 (2021) 342–352.
[42] J. Mittal, R. Ahmad, A. Mariyam, V.K. Gupta, A. Mittal, Expeditious and enhanced sequestration of heavy metal ions from aqueous environment by papaya peel carbon: a green and low-cost adsorbent, Desal. Water Treat., 210 (2021) 365–376.
[43] J. López-Luna, L.E. Ramírez-Montes, S. Martinez-Vargas, A.I. Martínez, O.F. Mijangos-Ricardez, M. del C.A. González-Chávez, R. Carrillo-González, F.A. Solís-Domínguez, M. del C. Cuevas-Díaz, V. Vázquez-Hipólito, Linear and non-linear kinetic and isotherm adsorption models for arsenic removal by manganese ferrite nanoparticles, SN Appl. Sci., 1 (2019) 950, doi: 10.1007/s42452-019-0977-3.
[44] R. Ahmad, I. Hasan, A. Mittal, Adsorption of Cr(VI) and Cd(II) on chitosan grafted polyaniline-OMMT nanocomposite: isotherms, kinetics and thermodynamics studies, Desal. Water Treat., 58 (2017) 144–153.
[45] S. Soni, P.K. Bajpai, D. Bharti, J. Mittal, C. Arora, Removal of crystal violet from aqueous solution using iron-based metal organic framework, Desal. Water Treat., 205 (2020) 386–399.
[46] G. Kiani, M. Dostali, A. Rostami, A.R. Khataee, Adsorption studies on the removal of malachite green from aqueous solutions onto halloysite nanotubes, Appl. Clay Sci., 54 (2011) 34–39.
[47] A. Ahmad, S.H.M. Setapar, A.A. Yaqoob, M.N.M. Ibrahim, Synthesis and characterization of GO-Ag nanocomposite for removal of malachite dye from aqueous solution, Mater. Today Proc., 47 (2021) 1359–1365.